2. DIFFRACTION GEOMETRY AND ITS PRACTICAL REALIZATION

the data by least squares in which the values of the derivatives can be calculated using a set of tabulated integers. The convolution range CR expressed as a multiple of the FWHM of the peak can be selected. A minimum of five points is required. For asymmetric peaks, such as occur at small 2θ's, a CR $\simeq 0.5$ FWHM gives the best precision. The larger the CR the larger the intrinsic error but the smaller the random error, and the smaller the number of peaks identified in overlapping patterns. The larger CR also avoids false peaks in patterns with poor counting statistics. Fig. 2.3.3.8(*c*) shows the dependence of the accuracy of the peak determination on P/σ. The computer results list the 2θ's, d's, absolute and relative intensities (scaled to 100) of the identified peaks. The calculation is made with a selected wavelength such as $K\alpha_1$ and the possible $K\alpha_2$ peaks are flagged.

2.3.3.8. *Profile fitting*

Profile fitting has greatly advanced powder diffractometry by making it possible to calculate the intensities, peak positions, widths, and shapes of the reflections with a far greater precision than had been possible with manual measurements or visual inspection of the experimental data. The method has better resolution than the original data and the entire scattering distribution is used instead of only a few features such as the peak and width. Individual profiles and clusters of reflections can be fitted, or the entire pattern as in the Rietveld method (Chapter 8.6).
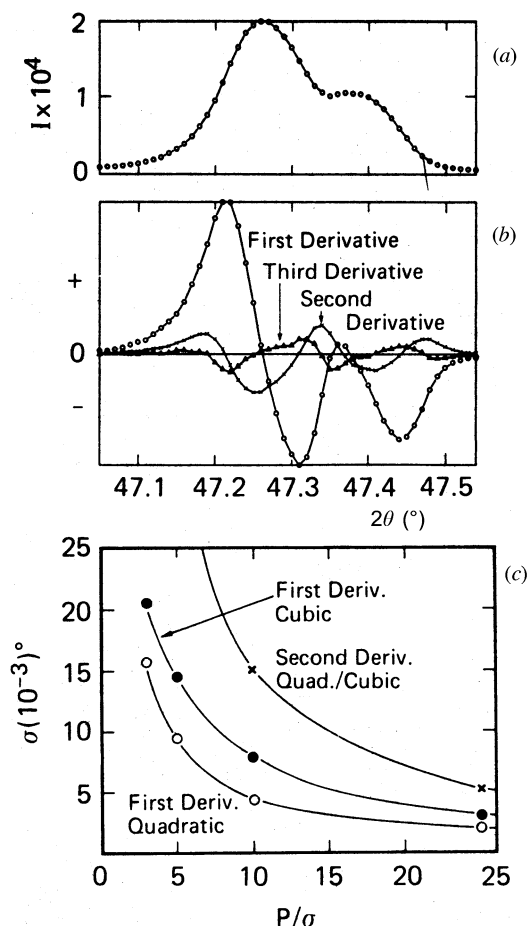
The procedure is based on the least-squares fitting of theoretical profile intensities to the digitized powder pattern. The profile intensity at the ith step is calculated by

$$Y(x_i)_{\mathrm{calc}} = B(x_i) + \sum_j I_j P(x_i - T_j)_j, \qquad (2.3.3.12)$$

where $B(x_i)$ is the background intensity, I_j is the integrated intensity of the jth reflection, T_j is the peak-maximum position, $P(x_i)_j$ is the profile function to represent the profile shape, and $\sum_j$ is taken over j, in which the $P(x)_j$ has a finite value at x_i. Unlike the Rietveld method, a structure model is not used. In the least-squares fitting, I_j and T_j are refined together with background and profile shape parameters in $P(x)_j$. Smoothing the experimental data is not required because it underestimates the estimated standard deviations for the least-squares parameters, which are based on the counting statistics.

The experimental profiles are a convolution of the X-ray line spectrum λ and all the combined instrumental and geometrical
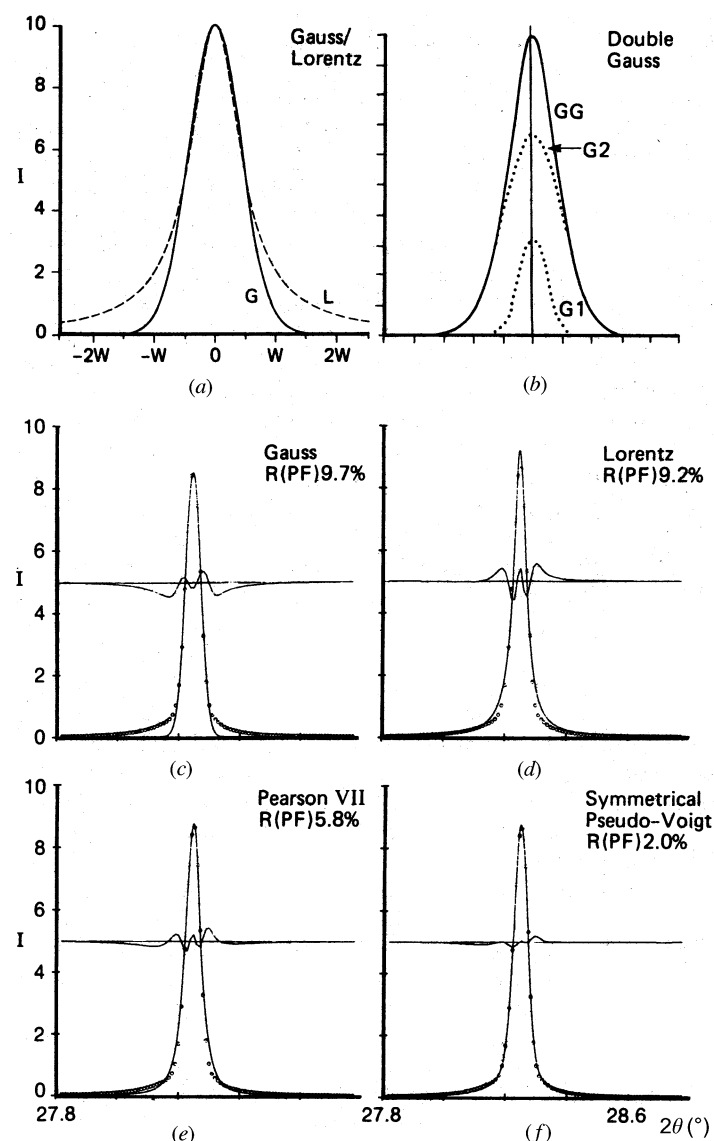

Fig. 2.3.3.8. (*a*) Si(220) Cu $K\alpha$ reflection. (*b*) First (circles), second (crosses), and third (triangles) derivatives of a seven-point polynomial of data in (*a*). (*c*) Average angular deviations as a function of P/σ for various derivatives.

Fig. 2.3.3.9. (*a*) Computer-generated symmetrical Lorentzian profile L and Gaussian G with equal peak heights, 2θ and FWHM. (*b*) Double Gaussian GG shown as the sum of two Gaussians in which I and FWHM of $G1$ are twice those of $G2$ and 2θ is constant. (*c*)–(*f*) Profile fitting with different functions. Differences between experimental points and fitted profile shown at one-half height. Synchrotron radiation, Si(111).

references